Biophysical Chemistry 142 (2009) 65–75

Contents lists available at ScienceDirect

Biophysical Chemistry

journal homepage: http://www.elsevier.com/locate/biophyschem

# Equivalence of $Mg^{2+}$ and $Na^{+}$ ions in salt dependence of the equilibrium binding and dissociation rate constants of *Escherichia coli* RNA polymerase open complex

Tomasz Łoziński, Krystyna Bolewska, Kazimierz L. Wierzchowski *

*Department of Biophysics, Institute of Biochemistry and Biophysics, Polish Academy of Sciences, Warszawa, Poland*

ARTICLE INFO

*Article history:*
Received 18 December 2008
Received in revised form 5 March 2009
Accepted 5 March 2009
Available online 14 March 2009

*Keywords:*
*Escherichia coli* RNA polymerase
Open transcription complex
$\lambda P_R$ promoter
Salt dependence of open complex stability
Effect of $Mg^{2+}$ on open complex stability

ABSTRACT

Conflicting experimental data on the influence of $Mg^{2+}$ ions on the salt dependence of formation/dissociation of open transcription complex (RPo) of *Escherichia coli* RNA polymerase led us to carry systematic measurements of the dissociation rate constant ($k_d$) and thermodynamic stability of complexes at $\lambda P_R$ and Pa promoters in a broad range of [NaCl] and [$MgCl_2$] at 25, 31 and 37 °C, using fluorescence detected abortive transcription assay. Values of $k_d$ determined in $MgCl_2$ in the presence of heparin, as a commonly used anionic competitor, were shown to depend on heparin concentration whereas in NaCl this effect was not observed. Kinetics of dissociation was therefore determined in the course of salt-induced down-shift of the binding equilibrium. Salt derivatives of $k_d$'s ($n_d$) appeared to be similar in NaCl (~8.5) and $MgCl_2$ (~10) for both complexes. Isotherms of fractional occupancy of promoters by RNAP as a function of ln [salt] were shown to conform to a sigmoid Boltzman function parameterized to include binding constant of RPo and a net change ($n_{obs}$) in the number of electrolyte ions associated with complex components upon its formation/dissociation. The fitted values of $n_{obs}$ appeared also similar in NaCl and in $MgCl_2$: ~18 for RPo/$\lambda P_R$ and ~20 for RPo/Pa, respectively. Overall unfavorable vant'Hoff enthalpy ($\Delta H_{obs}$) of RPo proved to be much higher in $MgCl_2$ than in NaCl by ca. 20 kcal/mol for both complexes, rendering them profoundly less stable in the former salt. In both salts, $\Delta H_{obs}$ was higher by ~30 kcal/mol for RPo/Pa relative to RPo/$\lambda P_R$. Similarity of $n_{obs}$ and $n_d$ values for the two salts indicates thermodynamic equivalence of $Mg^{2+}$ and $Na^{+}$ in [salt]-controlled binding equilibrium of RPo. This finding remains in disagreement with earlier data and suggests that salt effects on open complex stability should be sought in global compensating changes in distribution of all ionic species around the interacting complex components.



## 1. Introduction

The divalent magnesium cation is an essential element for the growth and maintenance of living cells, whose transport and role in cell homeostasis are extensively studied [1,2]. It is an essential cofactor required for catalytic function of a variety of enzymes, in particular for DNA and RNA polymerases [3,4]. However, the role of $Mg^{2+}$ ions in salt-controlled kinetics of initiation of transcription by bacterial RNA polymerase and in stability of open transcription complex is not well understood.

The major contribution to the free energy driving formation of transcription competent complexes by *Escherichia coli* RNA polymerase at cognate promoters in dilute salt solutions is of entropic origin connected primarily with a net change in the number of cations associated with negatively charged DNA phosphates [5–7]. The corresponding equilibrium binding constants of these complexes are thus strongly dependent on salt concentration. Kinetic experiments in NaCl have revealed that both the association ($k_a$) and dissociation ($k_d$) rate constants for the open transcription complex (RPo) of *E. coli* RNA polymerase (R) at the $\lambda P_R$ promoter (P) vary as $[Na^+]^{-12}$ and $[Na^+]^8$, respectively. Consequently, the corresponding equilibrium constant, $K_p = k_a / k_d$, varies with $[Na^+]^{-20}$ [8]. In dilute $MgCl_2$ solutions, this dependency has been reported to be very different for the association and dissociation reactions [6,9]: while $k_a$ varied as $[Mg^{2+}]^{-5}$, the value of $k_d$ appeared only very weakly [salt]-dependent, with an exponent of ca. 0.4. The latter observation has been interpreted as a net result of (i) reassociation of ca. 4 $Mg^{2+}$ ions (equivalent to 8 $Na^+$) upon renaturation of the melted promoter DNA to double-stranded form during RPo dissociation, and (ii) concomitant release of 3$Mg^{2+}$ ions from a postulated Mg-induced form of the complex called RPo2. In a similar study for RPo at a model Pa promoter [10], shown to conform like $\lambda P_R$ to the three-step mechanism of the complex formation [5,6,8], we have demonstrated that $k_d$ varies as $[Mg^{2+}]^4$. To resolve the apparent discrepancy between the two works, we extended our investigations on [salt]-dependence of the kinetics of dissociation of RPo at both $\lambda P_R$ and Pa

* Corresponding author. Department of Biophysics, Institute of Biochemistry and Biophysics, Polish Academy of Sciences, ul. Pawińskiego 5a, 02-106 Warszawa, Poland. Tel.: +48 22 592 2344; fax: +48 22 592 2190.
*E-mail address:* klw@ibb.waw.pl (K.L. Wierzchowski).

0301-4622/$ – see front matter © 2009 Elsevier B.V. All rights reserved.
doi:10.1016/j.bpc.2009.03.004

promoters to a broader range of [$MgCl_2$]. Parallel reference experiments were conducted in NaCl solutions. The reported herewith results of these studies demonstrate that: (i) heparin in the presence of $Mg^{2+}$ inactivates RPo in a bimolecular reaction so that it does not behave as a true polyanionic competitor that explains the discrepancy between the earlier measured values of [salt]-derivatives of $k_d$, and (ii) salt-derivatives of heparin-independent $k_d$'s in $MgCl_2$ and in NaCl are similar one with another. Subsequent determination of binding isotherms for RPo in the two salts at a number of temperatures allowed confirmation of the latter finding by showing that also [salt]-dependence of the binding equilibrium constant in the two salts is similar. Thermodynamic stability of RPo at both promoters appeared to much lower in $MgCl_2$ than in NaCl, however, owing to a higher unfavorable overall enthalpy of the complexes in the former solvent.

## 2. Experimental

### 2.1. RNA polymerase

RNA polymerase (EC 2.7.7.6) was prepared according to [11] as described previously [10,12,13]. The enzyme was stored at −20 °C in buffer S (50% glycerol, 100 mM NaCl, 10 mM Tris–HCl pH 7.9, 0.1 mM DTT); its activity was estimated according to [14] at ca. 50%. The enzyme concentrations reported here refer to its active form.

### 2.2. Promoters

Model promoter Pa was synthesized and cloned into pDS3 plasmid as described previously [12]; $\lambda P_R$ promoter, encompassing positions from −59 to +21 with respect to its transcription start site, was obtained by PCR [13] and cloned similarly into pDS3 plasmid. DNA fragments bearing promoter sequences: Pa (226 bp long) and $\lambda P_R$ (264 bp long) were prepared by PCR. Concentration of PAGE purified DNA fragments was determined spectrophotometrically. Sequences of the two promoters are shown in Scheme 1.

### 2.3. Reagents and chemicals

γ-ANS-UTP was prepared according to Yarbrough et al. [15]. ANS was from Fluka. UTP, ApA, CpA, heparin, Tris and 1.0 M solution of $MgCl_2$ were from Sigma. Poly(dT) was from Miles Laboratories. NaCl stock solution was prepared from dried salt (Chempur).

*Buffers*. Binding buffer (BB) used for RPo formation contained: 0.01 M Tris–HCl/pH 7.9, 0.001 M DTT, 0.01% BSA, and varying concentration of either NaCl (0.15–0.45 M) or $MgCl_2$ (0.05–0.13 M). For experiments in pure Tris–HCl buffer, pH 7.9, [Tris] was set at 0.225 M. Transcription buffer (TB) used for quantification of RPo in experiments carried out in the presence of NaCl contained: 0.01 M Tris–HCl/pH 7.9, 0.001 M DTT, 0.01% BSA 0.1 M NaCl, 0.01 M $MgCl_2$ and 10 μg/ml of heparin; in experiments conducted in $MgCl_2$ concentration of the latter salt in TB was 0.04 M, while when in pure Tris–HCl/pH 7.9 buffer–[Tris] was set at 0.15 M.

### 2.4. RPo formation

RPo complexes for equilibrium binding experiments were formed by incubating DNA fragment containing $\lambda P_R$ or Pa promoter (4 nM) and RNAP (40 nM) in the BB buffer 0.15 M in NaCl or 0.05 M in $MgCl_2$ for 2 h at 37 °C. These conditions were established with a reference to the published data [8,9], our laboratory experience [10] and results of the present work. They proved to be optimal for full occupancy of promoter DNA in the formation of both RPo/$\lambda P_R$ and RPo/Pa complexes. Higher [salt]'s in BB were used to set the binding equilibrium at a lower level of promoter occupancy. For kinetic studies the complexes were formed at a lower [RNAP]/[DNA] ratio of 4–5 and a smaller reactants concentration.

### 2.5. Modified fluorescence detected abortive initiation assay (MFDAI)

In order to be able to measure fast rates of RPo dissociation at high salt concentrations and to increase general accuracy of fluorescence detected abortive initiation assay (FDAI) [9,10], used for quantification of RPo at equilibrium, we modified this assay in the following way. A series of equilibrated RPo formation or dissociation reactions in BB buffer were sampled and immediately brought to TB buffer containing a lower [salt] and heparin (10 μg/ml), to prevent any changes in the original binding equilibrium, and substrates for abortive transcription initiation (final concentration: 0.2 mM in initiating dinucleotide, ApA or CpA respectively for RPo/Pa and RPo/$\lambda P_R$, and 0.1 mM in γ-ANS-UTP). The thus started steady-state transcription in the whole series of samples was carried out at 37 °C up to ca. 20% of consumption of the ANS-UTP substrate and then stopped by several-fold dilution with 0.02 M of EDTA solution. Finally, fluorescence intensity of accumulated fluorescent 5′-pyrophosphate-ANS product, proportional to content of RPo, was measured using earlier described dedicated spectrofluorimeter [10] and/or a microplate Fluorescence Reader (FLx Biotek). Control experiments showed that during the long lasting transcription reactions the extent of inactivation of RPo was very small and similar within the whole series of samples, so that relative content of RPo therein could be accurately determined.

### 2.6. Kinetics of RPo dissociation as a function of salt concentration

Dissociation of preformed open complexes in BB solution, equilibrated at a selected [salt] and temperature (25 or 37 °C, for RPo/$\lambda P_R$ and RPo/Pa, respectively), was initiated by the addition of an equal volume: (1) of a concentrated $MgCl_2$ or NaCl solution to a desired final [salt], to shift the binding equilibrium to a lower level (called salt-shift method), or/and (2) of a solution containing DNA competitor (heparin: 10–60 μg/mL, or poly(dT): 0.8 mg/mL), to make the reaction irreversible [9,10]. Fractions $f_{RPo}$ of open complexes remaining at time $t$ after initiation of dissociation process were determined using the MFDAI assay described in the preceding paragraph. The first-order dissociation rate constants $k_d$ were evaluated from linear least-squares fit (Origin 4.1) of the function: $\ln(f_{RPo}) = A + k_d \times t$ to the experimental $f_{RPo}$, (õ[salt], t) data points.

### 2.7. Determination of equilibrium fraction of RPo as a function of salt concentration

The amount of complexes formed in BB solution at a number of [salt]'s, or attained after shifting down the binding equilibrium by the addition of a concentrated salt solution to the binding reaction

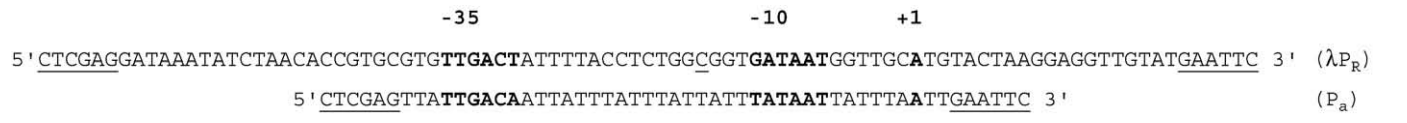


**Scheme 1.** Sequences (nontemplate strand) of the $\lambda P_R$ and $P_a$ promoters; within restriction sites (underlined) used for cloning into pDS3 plasmid. Transcription start site, −10 and −35 recognition hexamers are in bold font.

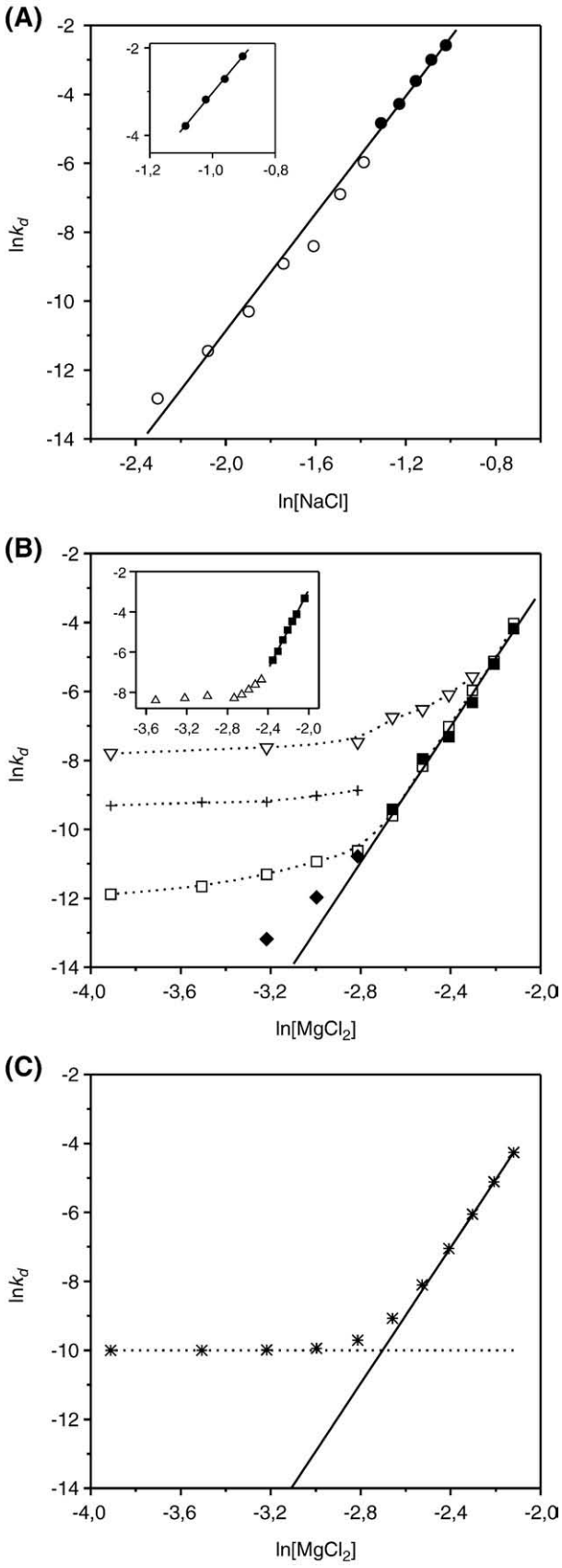


equilibrated at the optimal [salt], was determined with the help of the MFDAI assay at three selected temperatures: 25, 31 and 37 °C. In the latter case, equal volume aliquots were taken from a bulk solution containing preformed RPo at the optimal salt conditions, mixed with a series of BB solutions to set the final salt concentration (NaCl, $MgCl_2$, or Tris–HCl) at successively higher values. Reactions were then partitioned into three samples and each equilibrated for 6 h at the three different selected temperatures. Thereafter samples were diluted with salt solutions containing substrates to establish in all the samples of a given series the same standard conditions for transcription in TB buffer, appropriate for the MFDAI assay. Sigmoid plots of fluorescence intensity versus ln [salt] were first fitted to Boltzman function (using Origin 4.1) and then normalized yielding the sought $f_{RPo}$ (ln [salt],$T$) binding isotherms. The experimental procedure applied for the determination of the isotherms allows considering relative values of the fitted parameters as highly reliable.

## 3. Results

### 3.1. Dependence of the kinetics of RPo dissociation on salt concentration and heparin presence

First-order dissociation rate constants ($k_d$) for RPo/$\lambda P_R$ and RPo/Pa were determined as a function of [salt] in $MgCl_2$ and NaCl solutions by MFDAI assay (cf. Methods). The reaction was initiated either by the addition of heparin as a polyanionic competitor, or/and by the salt-shift method to bring the equilibrium $f_{RPo}$ to a lower value. Values of $k_d$ thus obtained in NaCl proved to increase single-exponentially as a function of [salt], so that plots of ln$k_d$ versus ln [salt] for both complexes in this salt were linear in the whole range of salt concentrations studied with a similar slope of $n_d \approx 8$ (cf. Fig. 1A and inset), independent of whether the reaction was initiated by the addition of heparin or by an increase in the salt concentration in the higher range of concentrations studied (cf. $f_{RPo}$ *vs.* ln[salt] isotherms in Figs. 3 and 4 below). In the lower range of [NaCl], an increase in [heparin] from 10 to 100 μg/mL had practically no effect on the measured $k_d$ value. The slope of the double logarithmic plot $n_d \equiv Sk_d = 7.7 \pm 0.2$ reported previously [8] for RPo/$\lambda P_R$ at 25 °C in a narrower range of [NaCl]: 0.19–0.27 M and in the presence of heparin, remains in a reasonable agreement with the one measured presently.

In $MgCl_2$, the pattern of double logarithmic plots of $k_d$([salt]) data (Fig. 1B) appeared quite different, however. In experiments in which the dissociation reaction of RPo/$\lambda P_R$ was initiated by the addition of a small amount of heparin (5 μg/mL), ln$k_d$ increased nonlinearly with ln[$MgCl_2$] in such a way that in the lowest range of salt concentrations (0.02–0.05 M) the slope of the plot was very small, $n_d \approx 0.3$, then it rose fast approaching a concentration independent value of $n_d \approx 10$ between ca. 0.07 and 0.12 M $MgCl_2$. Moreover, when the kinetics of reaction was studied in the latter range of [$MgCl_2$] by the salt-shift method in the absence of heparin, the plot was practically linear with the same value of

**Fig. 1.** Double-logarithmic plots of the dissociation rate constant, $k_d$, as a function of [NaCl] (A) and [$MgCl_2$] (B) in BB buffer for RPo/$\lambda P_R$ at 25 °C (main panels) and RPo/Pa at 37 °C (insets). Dissociation rates were measured in the high [salt] region in the absence of a competitor by [salt]-shift method (filled rectangles and circles); and in the lower [salt] region in the presence of competitors: heparin: at 5 mg/L (open rectangles). 10 mg/L (open circles), 5–15 mg/L (crosses, data taken from [9]), 25 mg/L (open uptriangles) and 60 mg/L (open downtriangles), and poly(dT) at 800 mg/L (filled diamonds). Data points are mean values from 2 to 3 independent measurements; corresponding standard errors, comparable with the symbol's size, are not shown for clarity, solid lines — fitted linear functions, for RPo/$\lambda P_R$: $\ln k_d = 6.16 (\pm 0.21) + 8.52(\pm 0.14) \times \ln[NaCl]$ and $\ln k_d = 16.62(\pm 1.19) + 9.85(\pm 0.53) \times \ln[MgCl_2]$, for RPo/Pa: $\ln k_d = 5.58(\pm 0.43) + 8.58(\pm 0.42) \times \ln[NaCl]$ and $\ln k_d = 16.63(\pm 0.28) + 9.79(\pm 0.13) \times \ln[MgCl2]$. (C): Plot of the calculated function $k_{d,obs} = k_d + k_{d,hep}$ [Hep] (asterisks), using ($k_d$,[$MgCl_2$]) data from panel B (solid line) and $k_{d,hep}$ value at 10 mg/L heparin from Fig. 2 (dotted line).

$n_d \approx 10$. The plot of $\ln k_d(\ln[MgCl_2])$ data of Suh et al. [9], measured in 0.02–0.06 M range of $[MgCl_2]$ at 5–15 μg/mL of heparin (assumed mean value 10 μg/mL), is similar in shape but corresponding $k_d$ values are higher by one order of magnitude than those determined by us at 5 μg/mL of heparin (cf. Fig. 1B). To get a better insight into the mechanism of this heparin effect on the kinetics of RPo dissociation we measured $k_d$ as a function: (1) of $[MgCl_2]$ at a much higher heparin concentration of 60 μg/mL, and (2) of [heparin] at a selected constant $[MgCl_2] = 0.04$ M. The shape of the double logarithmic plot of the data set from the first experiment (Fig. 1B) is similar to that obtained at 5 μg/mL of heparin except that the whole plot is shifted up to higher $\ln k_d$ values corresponding to much faster kinetics of RPo dissociation than that observed both at 5 and 10 μg/mL of heparin. The second experiment demonstrated that $k_d$ increases linearly with heparin concentration (cf. Fig. 2). These results clearly indicated that heparin in $MgCl_2$ solutions does not behave as a true polyanionic competitor in the process of RPo dissociation. In early heparin challenge kinetic transcription initiation experiments [16–19], in addition to the true dissociation of initiated complexes also their inactivation by heparin in a bimolecular attack have been observed. This seemed to be the case in our experiments. Indeed, the observed dissociation rate constant could be represented as a sum of two components, *i.e.* $k_{d,obs} = k_d + k_{d,hep}[Hep]$. The nonlinear $\ln k_{d,obs}$ vs. $\ln[MgCl_2]$ plots could be dissected into two linear functions, as exemplified in Fig. 1C, one representing the true heparin-independent dissociation ($k_d$) extrapolated to lower[salt]'s, and a [heparin]-dependent one corresponding to the inactivation of RPo by bimolecular heparin attack ($k_{d,hep}[Hep]$). In the lower range of $[MgCl_2]$, $k_d \ll k_{d,hep}[Hep]$ so that observed reaction is dominated by heparin attack on RPo. Owing to the strong [salt]-dependence of the true dissociation reaction it becomes dominant at higher concentrations of the salt.

Experiments with the use of poly(dT) as an anionic competitor demonstrated ultimately that RPo/$\lambda P_R$ dissociation also at low $MgCl_2$, *i.e.* between 0.02 and 0.06 M, is characterized by a similar value of $n_d$ to that observed in the higher range of salt concentrations (cf. corresponding data points in Fig. 1B).

The results of kinetic experiments on RPo/Pa dissociation in $MgCl_2$ appeared generally similar to those on RPo/$\lambda P_R$, both in the presence and in the absence of heparin, (cf. insets in Fig. 1B). The $n_d$ values for RPo/Pa in both salts were also found closely similar to those determined for RPo/$\lambda P_R$. Since the experiments for RPo/Pa and RPo/$\lambda P_R$ were carried out at different temperatures of 37 and 25 °C, respectively, similarity of the corresponding $n_d$ values indicates that they can be regarded practically independent of temperature, as it has been observed previously for RPo/Pa [10].

The presented results fully explain the apparent discrepancy between the earlier determined slopes of double logarithmic plots of $k_d([MgCl_2])$ data for the two complexes [9,10] as due to different heparin and $MgCl_2$ concentrations. More importantly, they demonstrate unequivocally that heparin-independent [salt]-dependency of $k_d$ for RPo is similar in $MgCl_2$ and in NaCl.

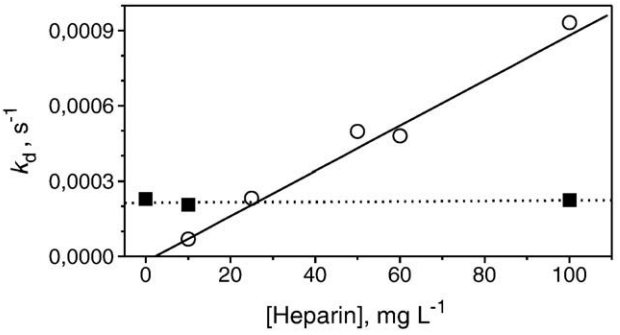


**Fig. 2.** Effect of heparin on the dissociation rate constant, $k_d$, of RPo/$\lambda P_R$ at 25 °C. Measured as a function of [heparin] in 0.04 M $MgCl_2$ (open circles), and in 180 mM NaCl (filled rectangles).

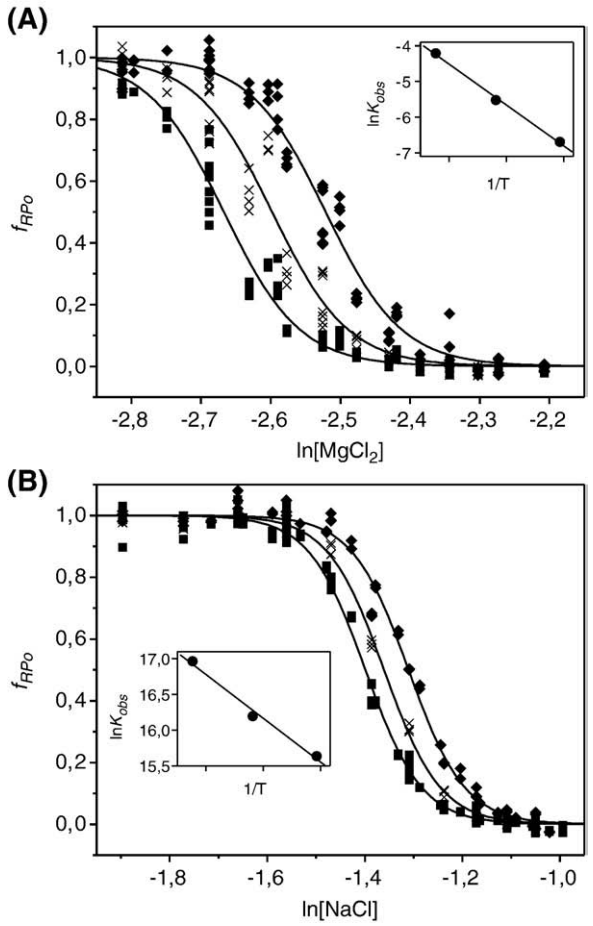


**Fig. 3.** Binding isotherms for RPo formation at $\lambda P_R$ promoter by *E. coli* RNA polymerase. (A) In $MgCl_2$ and (B) in NaCl at 25 (filled rectangles), 31 (crosses) and 37 °C (filled diamonds), and corresponding vant'Hoff plots (insets). Fractional promoter occupancy ($f_{RPo}$,[salt],$T$), measured with the help of the MFDAI assay, was shifted down by successive addition of salts to preformed RPo in BB buffer at optimal salt conditions. Solid lines represent a modified sigmoid Boltzman function (Eq. (1)), the fitted parameters of which are collected in Table 1. Values of the apparent binding constants $K_{obs}$ for linear vant'Hoff plots (in insets, average correlation coefficient 0.995) were calculated for 0.1 M salts and 40 nM polymerase using Eq. (2) and corresponding fitted $\ln K$ and $n_{obs}$ parameters from Table 1; calculated $\Delta H_{obs}$ values in Table 1.

### 3.2. Dependence of the thermodynamic stability of RPo on salt concentration

Open complexes at the $\lambda P_R$ and Pa promoters were preformed in the binding buffer at optimal salt and temperature conditions for each promoter and 10-fold excess of RNAP at which the equilibrium fraction of RPo reached $f_{RPo} \sim 1$ (full occupancy of promoter DNA). They were then exposed to successively higher salt concentrations (salt-shift) of either NaCl (0.15–0.45 M) or $MgCl_2$ (0.06–0.13 M) at three selected temperatures (25, 31 and 37 °C) for sufficient period of time to bring the equilibrium amount of RPo to a lower value. Alternatively, the complexes were formed at the same final [salt] in the binding buffer. The equilibrium amount of RPo at each [salt] was quantified using the MFDAI assay described in the Experimental section. The thus obtained sigmoid binding isotherms: $f_{RPo} = F(\ln[salt],T)$, conforming to Boltzman function, are shown in Figs. 3 and 4. The isotherms obtained by the use of either of the two alternative methods of bringing the system to the

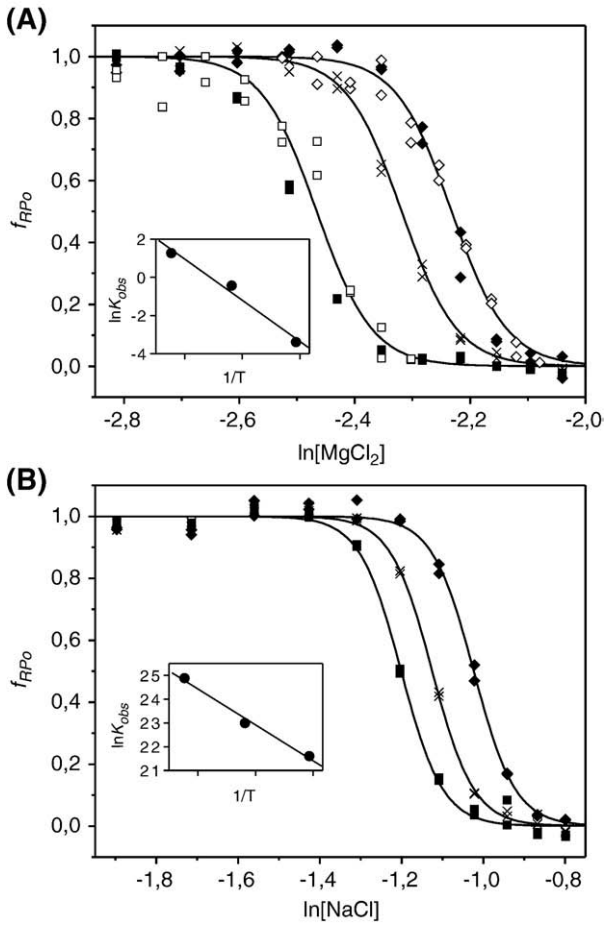


**Fig. 4.** Binding isotherms for RPo formation at Pa promoter by *E. coli* RNA polymerase. (A) In $MgCl_2$ and (B) in NaCl at 25 (filled rectangles), 31 (crosses) and 37 °C (filled diamonds), and corresponding vant'Hoff plots (insets). Experimental details as in the legend to Fig. 3, except for that additional open symbols denote ($f_{RPo}$,[salt],$T$) data points obtained by RPo formation at corresponding [salt].

equilibrium at a given [salt] proved to be similar, as exemplified in Fig. 4A (cf. filled and open symbols). Therefore, in most experiments the more convenient experimentally salt-shift method was used.

The sigmoid form of the isotherms reflects the dependence of the equilibrium constant of RPo: $K_{eq} = \frac{[RPo] \times [Me^{+/++}]^{n_C} \times [A^-]^{n_A}}{[RNAP] \times [DNA]}$, on salt concentration and $n_{obs} = n_C + n_A$ – the net change in the number of electrolyte ions associated with the free and bound complex components upon RPo formation/dissociation ($n_C$ and $n_A$ are not equal necessarily). The Boltzman function was thus appropriately parameterized to include these quotients, as described in the Appendix A (cf. Eq. (A11)):

$$f_{RPo} = \frac{1}{1 + e^{(n_{obs} \times \ln[salt] - \ln K)}} \quad (1)$$

where $\ln K = \ln K_{eq} + \ln[RNAP]$, $K_{eq}$ corresponds to $K_{obs}$ extrapolated to 1.0 M salt, abbreviated as $K_{obs,1.0\ M}$. Under experimental conditions such that [RNAP] ≫ [DNA] (as in this work where [RNAP]/[DNA] = 10]), concentration of RNAP can be assumed constant in the whole range of $f_{RPo}$ values (for assessment of possible errors caused by this assumption see Appendix A). Global fits of the $f_{RPo}(\ln[salt],T)$ data for a given complex and salt were performed assuming that the parameter $n_{obs}$ does not depend on temperature (cf. representative plots and fits in Figs. 3 and 4). This assumption is well justified since the general structure and the extent of open region in RPo do not change in the studied narrow temperature range of 25–37 °C [10,13]. Values of the fitted parameters: $\ln K$ and $n_{obs}$, and of the corresponding $\ln K_{eq}$ calculated using known [RNAP] = 40 nM, are collected in Table 1. Salt concentration, $x_0$, at which $f_{RPo} = 0.5$, characteristic for salt stability of RPo at a specified RNAP concentration (obtained either by fitting of the classical Boltzman function to $f_{RPo}(\ln[salt],T)$ data or calculated from the relationship $\ln K / n_{obs} = \ln(x_0)$, are also collected in Table 1. Since pH of Tris–HCl buffered salt solutions decreases with a rise in temperature (but negligibly with [salt]) [20], the fitted values of $\ln K$ at 304 and 310 K, had to be corrected for this pH-effect before calculation of thermodynamic parameters. For this purpose a series of isotherms $f_{RPo}(\ln[salt],pH)$ for the RPo/λP$_R$ in pH range of 7.6–8.2 was measured in both salts (data not shown) wherefrom the sought common relationship: $d\ln K / d(pH) = -0.57$ ($\ln K_{NaCl} = -19.5(\pm 0.9) - 0.57(\pm 0.12) \times pH$) was determined and the fitted values of $\ln K$ at 304 and 310 K corrected for by −0.1 and −0.2 units, respectively.

Since binding isotherms were obtained in the presence of Tris buffer it was necessary to evaluate also the effect of its concentration on RPo stability. Therefore, the binding isotherm for RPo/λP$_R$ in pure Tris buffer (pH 7.9) at 25 °C was measured (data not shown) and the corresponding parameters determined: $x_0 = 0.259$ M, $n_{obs} = 21.8$,

**Table 1**
Binding equilibrium and thermodynamic parameters calculated by fitting experimental isotherms: $f_{RPo} = F(\ln[salt],T)$ (Figs. 3 and 4) to Boltzman function (Eq. (1)).

| Complex → | RPo/λP$_R$ | | | RPo/Pa | |
|---|---|---|---|---|---|
| Parameter, (units) | $T$, K | NaCl | $MgCl_2$ | NaCl | $MgCl_2$ |
| $x_0$, (M) | 298 | 0.247 | 0.0694 | 0.301 | 0.0849 |
| | 304 | 0.255 | 0.0740 | 0.323 | 0.0979 |
| | 310 | 0.267 | 0.0795 | 0.356 | 0.1063 |
| $n_{obs}$ | | 17.30 (0.39) | 18.34 (0.80) | 19.61 (0.79) | 20.78 (1.17) |
| $\ln K^a \equiv \ln K_{eq} + \ln[RNAP]$ | 298 | −24.20 (0.55) | −48.92 (2.11) | −23.55 (0.95) | −51.24 (2.88) |
| | 304 | −23.64 (0.54) | −47.75 (2.06) | −22.16 (0.89) | −48.28 (2.71) |
| | 310 | −22.87 (0.52) | −46.44 (2.00) | −20.27 (0.81) | −46.58 (2.60) |
| $\ln K_{eq} \equiv K_{obs,1.0\ M}$ | 298 | −7.16 | −31.88 | −6.52 | −34.20 |
| | 304 | −6.60 | −30.72 | −5.13 | −31.25 |
| | 310 | −5.83 | −29.40 | −3.24 | −29.55 |
| $\Delta G_{obs,1.0\ M,\ T}$, (kcal/mol) | 298 | 4.24 | 18.88 | 3.86 | 20.26 |
| | 304 | 3.99 | 18.56 | 3.10 | 18.88 |
| | 310 | 3.59 | 18.11 | 1.99 | 18.08 |
| $\Delta H$, (kcal/mol) | | 20.4 (2.1) | 38.0 (1.7) | 50.45 (6.6) | 71.1 (8.0) |
| $\Delta S_{obs,1.0\ M}$, (e.u.) | | 54.0 | 64.0 | 156.4 | 170.6 |

In brackets standard errors returned from the fits using Marquard minimization algorithm.

[a] Values at 304 and 310 K corrected by −0.1 and −0.2 units, respectively; due to the decrease of Tris–HCl buffer pH at 298 K by 0.15 and 0.3 units at the two higher temperatures, the necessary corrections were obtained from the relationship: $d\ln K / dpH = -0.57$, determined from a series of experimental $f_{RPo}(\ln[salt],pH)$ isotherms of RPo/λP$_R$.

**Table 2**
Salt-dependent parameters $n = d\ln X / d\ln[salt]$ of experimentally determined equilibrium, $K_{obs}$, and dissociation rate constants, $k_d$, and of corresponding calculated association rate constants $k_a$ ($n_a = n_{obs} - n_d$) for RPo/λP$_R$ and RPo/Pa complexes at 25 °C.

| | NaCl (0.15–0.45 M) | | | $MgCl_2$ (0.06–0.13 M) | | |
|---|---|---|---|---|---|---|
| | $n_{obs}$ | $n_d$ | $n_a$ | $n_{obs}$ | $n_d$ | $n_a$ |
| RPo/λP$_R$ | −17.3 (0.4)[a] | 8.5 (0.1)[a] | −8. 8 (0.5)[a] | −18.3 (0.8) | 9.9 (0.5) | −8.4 (0.9) |
| RPo/Pa | −19.6 (0.8) | 8.6 (0.4)[b] | −11.0 (1.0) | −20.8 (1.2) | 9.8 (0.1)[b] | −11.0 (1.2) |
| $\Delta n$ (λP$_R$ − Pa) | 2.3 (0.9) | −0.1 (0.4) | 2.2 (1.1) | 2.5 (1.4) | 0.1 (0.5) | 2.5 (1.5) |

In brackets standard errors at 0.95 confidence coefficient (as in Table 1) or calculated (for $n_a$ and $\Delta n$'s) as a square root of the sum of individual $\sigma^2$ values.
[a] Roe and Record [8] using different experimental conditions (0.01 M sodium HEPES buffer pH 7.5) and filter binding assay have found for RPo/λP$_R$ in NaCl: $Sk_p \equiv n_{obs} = -19.6$ (1.3), $Sk_d \equiv n_d = 7.7$ (0.2) and $Sk_a \equiv n_a = -11.9$ (1.1), in a reasonable agreement with the present data.
[b] Determined at 37 °C, independent of temperature between 25 and 37 °C.

$\ln K = -29.5$. Equivalent NaCl and $MgCl_2$ concentrations of 10 mM Tris buffer (pH 7.9, 70% $Tris^+$) were calculated from the ratio of the corresponding $x_0$ values: 7 and 2 mM, respectively, small enough to be neglected. Both salts have a common $Cl^-$ anion so that it can be concluded that $Na^+$ and $Tris^+$ ($^+N(CH_2OH)_3$) contribute almost equally to RPo stability. Capillary affinity electrophoresis data on mobility of dsDNA in different buffers [21] led the authors to a similar conclusion, that $Tris^+$ ions are associated with DNA to approximately the same extent as sodium ions.

Calculation of equilibrium constants using Eq. (2) (cf. A12 in Appendix A):

$$\ln K_{obs,[MeA],T} = \ln K_{eq,T} - n_{obs} \times \ln[salt] = \ln K_T - \ln[RNAP] - n_{obs} \times \ln[salt] \quad (2)$$

allowed evaluation of the salt-dependent thermodynamic parameters from linear relationships: $\Delta G_{obs,T} = \Delta G_{obs,1.0\ M,T} + (R \times T \times n_{obs} \times \ln[salt])$ and $\Delta S_{obs} = \Delta S_{obs,1.0\ M} - (R \times n_{obs} \times \ln[salt])$ the values of which extrapolated to 1.0 M salts ($R$ — gas constant, $T$ — temperature in K), $\Delta G_{obs,1.0\ M,T}$ and $\Delta S_{obs,1.0\ M}$, are collected in Table 1. The [salt]-independent enthalpy values, $\Delta H_{obs}$, were calculated from vant'Hoff plots (cf. insets in Figs. 3 and 4). Independence of $\Delta H_{obs}$ on [salt] is a consequence of the assumption that $n_{obs}$ does not depend on temperature. In view of a good fit of the linear vant'Hoff equation to $\ln K_{obs,T}$ data (average correlation coefficient: 0.995) the thus obtained $\Delta H_{obs}$ values could be regarded temperature-independent in the studied narrow temperature range of 25–37 °C.

Earlier estimation of enthalpy for RPo/λP$_R$ [22] was based on the determination of Arrhenius enthalpies of activation for $k_a$ and $k_d$ in a broader temperature range of 13–37 °C, and calculation there from of $K_{obs} = k_a / k_d$ and of the corresponding temperature-dependent vant'Hoff enthalpies. The limited experimental $K_{obs}$ data available for 25–37 °C range (two data points only) [22] allowed only rough estimation of the overall ΔH for RPo as ca. 15 kcal/mol. The latter value remains in a reasonable agreement with the presently determined value of 20.4 kcal/mol.

## 4. Discussion

The most important novel findings of this work are: (i) the close similarity of [salt]-derivatives of RPo dissociation rate constant ($n_d$) and equilibrium binding constant ($n_{obs}$) in $MgCl_2$ and NaCl solutions, (ii) the much larger and independent of the promoter sequence overall enthalpy of RPo formation in $MgCl_2$ than in NaCl, rendering the complex much less stable thermodynamically in the former salt, (iii) the much larger overall enthalpy of RPo at Pa than at λP$_R$ promoter in both salts, adding strength to earlier indications of the dependence of this thermodynamic function on promoter sequence, and (iv) the demonstration that heparin in the presence of $Mg^{2+}$ does not behave as a true polyanionic competitor of DNA in RPo dissociation.

We shall comment on each of these points below in the context of the pertinent experimental data and interpretations of salt effects on RPo and some other protein–DNA complexes.

### 4.1. Similarity of [salt]-derivatives of dissociation rate and equilibrium binding constants of RPo in $MgCl_2$ and NaCl

We did not measure directly the kinetics of RPo formation, nevertheless [salt]-derivatives of this process at equilibrium, $n_a$, could be deduced from the relationship: $n_a = n_{obs} - n_d$ (as $d\ln K_{obs} / d\ln[salt] = d\ln\ln k_a / d\ln[salt] - d\ln\ln k_d / d\ln[salt]$) using the experimental $n_{obs}$ and $n_d$ values (cf. Tables 1 and 2). For RPo/λP$_R$ one obtains $n_{a,NaCl} \approx n_{a,\ MgCl_2} \approx -9\ (\pm 1)$. We are conceived that the earlier reported lower value of $n_a \equiv Sk_a = -5.2(\pm 0.3)$ for RPo/λP$_R$ in $MgCl_2$ [9] was underestimated owing to rather scanty experimental evidence (three data points only in a narrow [$MgCl_2$] range). The demonstrated similarity of [salt]-dependencies in NaCl and in $MgCl_2$ for $k_d$ and $K_{obs}$ and the deduced $n_a$ values for $k_a$ can be summarized in the well documented three-step minimal mechanism of open complex formation [5,6,8,23–26], as shown in Scheme 2.

Similarity of $n_d$ values has provided ultimate proof that the hypothetical fourth step in this mechanism [5,9], postulating conversion of $I_2$ into a final form of open complex, RPo2, upon binding of 3 $Mg^{2+}$ to a partially opened RPo1 intermediate, can be definitely omitted in this scheme. Alleged $Mg^{2+}$-induced extension of the transcription bubble underlying this hypothesis [27] has been disproved earlier by several independent lines of evidence [10,13,28,29].

For RPo/λP$_R$ similar values of respective $n_a \equiv Sk_a$, $n_d \equiv Sk_d$ and $n_{obs} \equiv Sk_p$ parameters in NaCl and sodium acetate (NaOAc) [9] as well as of $n_a \equiv Sk_a$, in potassium glutamate (KGlu) [30] were previously reported. It should be recalled in this connection that also replacement of $Na^+$ by a much larger in size $Tris^+$ cation (Tris[hydroxymethyl]-aminomethane$^+$) had only a small effect on $n_{obs}$ (cf. Results and Table 2). All these parameters resemble in magnitude those found in this work for the same complex in NaCl and $MgCl_2$. Therefore, [salt]-derivatives of the kinetic and equilibrium parameters of RPo can be regarded independent of both cations and anions nature.

According to polyelectrolyte theory [5], in solutions containing a single species of cation, it is the valence of the latter which determines primarily [salt]-dependence of the observed equilibrium binding and kinetic constants of formation/dissociation for DNA–protein complexes. These predictions are consistent with the results of experimental studies on monovalent [salt]-dependence of the equilibrium constant for binding of z-valent oligolysines and oligoarginines to double- and single-stranded nucleic acids [31–33]. Different anions (fluoride, acetate, chloride,) were found to exert only a small effect on

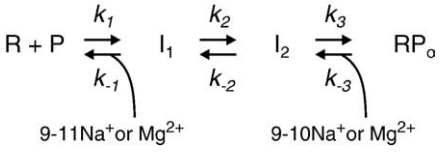


**Scheme 2.** Three step mechanism of RPo formation/dissociation.

this derivative the magnitude of which correlated with anions' position in the Hoffmeister series [6]. Also a simple model protein–DNA system of λ phage *lac* repressor–operator DNA complex conforms to the polyelectrolyte interpretation since the N-terminal headpiece of the repressor binds to the operator sequence as an octacation with the release of $Na^+$ or/and $Mg^{2+}$ ions in 2:1 stoichiometry [34,35].

The currently demonstrated independence of cations' valence of salt dependency of the kinetic and equilibrium parameters for RPo distinguishes this complex from simpler DNA–protein systems referred to above. In RPo, promoter DNA and RNAP form an extensive interface involving a large number of specific (−35 and −10 recognition hexamers and 14 bp transcription bubble) and nonspecific contacts (most of 17 bp linker and downstream dsDNA) involving altogether at least 60 bp [7]. At a first sight, one could thus expect that the salt dependence of kinetic and equilibrium parameters for RPo should be dominated by the polyanionic properties of DNA. This is apparently not the case, however. It is thus obvious that the salt-dependent properties of RPo can hardly be explained solely in terms of polyelectrolyte effect emphasizing the role of DNA and local salt-dependent interactions.

Results of application of nonlinear Poisson–Boltzmann (NLPB) model with added salts [36] to description of salt-dependent DNA–protein interactions seem to provide clues for understanding of the similarity of NaCl and $MgCl_2$ effects on RPo binding equilibrium. In this model, the counterion atmosphere around a polyion is treated as a single population of continuously distributed salt-dependent ion atmosphere resulting from long-range electrostatic interactions. Finite-difference NLPB calculations of the salt-dependent contributions to the electrostatic binding free energy of λcl repressor and *Eco*R1 endonuclease [37] with cognate DNA sequences have amply demonstrated that changes in the global pattern of cations and anions distribution accompanying formation of these complexes are responsible for the observed salt effects. Moreover, subsequent NLPB calculations of the electrostatic binding free energy of the λcI repressor–$O_L$I complex in pure NaCl and $MgCl_2$ salts [38] have shown that the total free energy of binding in the two salts varies linearly with log[salt] with similar correlation coefficients ($m_{bind}$) of 3.89 and 3.29, respectively. Since composite salt effects of all ionic species in solution underlie $m_{bind}$, the authors argue that value of this parameter is a sensitive function of the charge distribution of the interacting molecules but not of the valence of the binding ligand. A significant contribution to $m_{bind}$ was shown to be due to the $m_{lig}$ constituent characterizing salt dependence of the free energy of interaction of the repressor with its own ionic atmosphere, strongly dependent on $Cl^-$ concentration. This finding stressed importance of anion–protein interactions in the overall salt dependence of the binding process. A deeper insight into the role of long-range electrostatic interactions in nucleic acid–protein complexes was provided by recent experimental and NLPB modeling studies [39] on a model complex, of known NMR structure [40], made of a small α-helical peptide from the λ phage N protein and its cognate box B RNA hairpin. They showed that all the 12 positive and negative peptide charges up to 11A from backbone phosphate groups contribute significantly to the electrostatic free energy of RNA binding, while only a subset of positively charged groups remains in a close contact with RNA phosphates. They have indicated also that anion release contributes to salt dependence of this complex formation.

Results of the studies referred to above allow us to propose that explanation of the independence of cation's valence of the observed salt effects on RPo kinetic and equilibrium binding parameters should be sought according to the NLPB model in global changes in the distribution of ions in the field of long-range electrostatic interactions upon complex formation/dissociation. Inspection of the present model of RPo structure [41], based on low resolution crystal structure of *Thermus aquaticus* RNA polymerase holoenzyme complexed with a fork-junction promoter DNA fragment, in connection with the high resolution structure of *Thermus thermophilus* RNA polymerase elongation complex [42] provides arguments in favor of our proposal.

For interpretation of the $n_d$ values it was of interest to estimate the number of potential ionic contacts between various regions of RNAP and promoter template and nontemplate DNA phosphates. In the RPo model [41], the nontemplate channel RNAP regions σ2.1 and 2.3 provide a strip of four positively charged residues (corresponding to $Arg^{385}$, $Lys^{392}$, $Lys^{393}$ and $Arg^{426}$ of *E. coli* RNAP) potentially positioned to interact with DNA phosphates between −5 and −2 positions. Also $Arg^{99}$ of σ 1.2 region could contact the backbone of nontemplate DNA strand between the −10 element and the transcription start site, as it has been suggested recently [43]. At the entrance to the template strand channel a cluster of four universally conserved basic amino acids ($Arg^{436}$, $Lys^{462}$, $Arg^{465}$ and $Arg^{468}$ in *E. coli* enzyme) which may contribute to the electrostatic potential directing this strand into the tunnel is located. Since the presence of $Mg^{2+}$ ions does not influence the size of transcription bubble [10,13,29,44], the somewhat larger $n_d$ value in $MgCl_2$ than in NaCl (at most by ca. 1, cf. Tables 1 and 2) may indicate the formation of an additional $Mg^{2+}$-mediated ionic contact(s) between template DNA strand and the NADFDGD Mg-binding motif of RNAP within the RPo catalytic site [41]. The number of direct ionic contacts between DNA phosphates and basic RNAP groups that could be formed upon promoter DNA melting ranges thus between 8 and 10, formally in close correspondence with the experimental $n_d$ values. The number of the positively charged groups in RPo protein channels is far from sufficient, however, to neutralize all the 24–28 negative ssDNA charges. Possible explanation of how most of these charges could be neutralized in protein channels comes from the recent high resolution crystallographic study of the elongation complex of *T. thermophilus* RNAP [42]. It has been shown namely that the 13 bp long downstream DNA duplex is stabilized in the protein channel (made by β,β′-pincer's) elements through long-distance electrostatic interactions with very few direct polar contacts. Similarly, both short- and long-distance interactions with basic amino groups can thus be held responsible for stabilization of the separated ssDNA strands in the open complex. Negative phosphate charges can be also neutralized by electrolyte counterions able to penetrate the highly dynamic structure of RPo. This has been demonstrated indirectly by showing that kinetics of $MnO_4^-$ oxidation of thymine bases within the transcription bubble of RPo in the presence of low $Mg^{2+}$ concentration becomes faster in a position-dependent manner [13], owing to more efficient screening of DNA phosphate charges by divalent than monovalent ions. $Mg^{2+}$ ions were also shown to mediate the interaction of newly synthesized RNA with RNAP in the RNA exit channel in the elongation complex [42]. Formation of RPo requires also a shift of the highly negatively charged σ1.1 region (net charge −13) from its position in the holoenzyme between β and β′ pincers, destined to hold the downstream DNA duplex, to a new location on the highly positively charged domain (lobe 1of β pincer) [24,42,45,46]. This rearrangement, known to influence the rate of RPo formation [47], can be expected to contribute to the [salt]-dependence of RPo formation/dissociation. Similar opening of specific binding sites for ssDNA and dsDNA has been shown to occur in T4 gene 32 and T7 gene 2.5 proteins by salt-dependent removal of their negatively charged C-terminal domains from original locations [48–50].

All these considerations indicate that salt-dependent properties of RPo are most probably due to the dominance of long-range electrostatic interactions involving complex components and, consequently, also all the ionic species in solution. We are thus tempted to propose that the independence of the cations' valence of $n_{obs}$ and $n_d$ parameters can be regarded as a thermodynamic signature of involvement of such interactions. Quantitative verification of this hypothesis should be sought within frameworks of the NLPB model [36–38] when a high resolution structure of the complex will be available.

### 4.2. Mg-effect on thermodynamic stability of RPo

Although the [salt]-dependence of the kinetics of RPo formation/dissociation is shown to be independent of the electrolyte nature, the

latter exerts a profound effect on the thermodynamic stability of RPo. Comparison of the isotherms (Figs. 3 and 4) and related thermodynamic parameters in Table 1 leads to a number of quantitative observations concerning effects of electrolyte nature on thermodynamic stability of the open transcription complex.

In terms of $x_0$, that is at a salt concentration at which free energy of RPo attains the same value independent of the promoter structure and electrolyte nature, the complex at the both promoters studied is profoundly more stable in NaCl then in $MgCl_2$: $x_{0,298}$ in NaCl lies at 3.5-fold higher salt concentration than in $MgCl_2$. This means that RPo in $MgCl_2$ is practically nonexistent in that range of [salt]'s in which it is still stable in NaCl.

Analysis of thermodynamic parameters indicates that the salt-dependent equilibrium between RPo and its components is entropy driven, in agreement with earlier observations [5,6,8], and provides explanation of the large differences in RPo stability between NaCl and $MgCl_2$. The generally large and unfavorable $\Delta H_{obs}$ is more than compensated by the $T\Delta S_{obs,[salt]}$ term, which decreases with increasing [salt]. The increase of $|\Delta G_{obs,[salt],T}|$ in the studied range of 298–310 K is solely due to the rise in temperature bringing the $T\Delta S_{obs,[salt]}$ term to a larger value. Plots of the experimental $\Delta G_{298} = -RT\ln K_{obs}$ data as a function of ln[salt] for RPo/$\lambda P_R$ (Fig. 5) in NaCl (this work and [8]), in NaOAc [9] and in $MgCl_2$ (this work) indicate that at 0.1 M salt, $\Delta G_{298} = -6.3$ kcal/mol in $MgCl_2$, triplicates in NaCl to −19.1 kcal/mol (23.2, [8]) and quadruplicates up to −28.2 kcal/mol in NaOAc. The distinctly lower stability of RPo/$\lambda P_R$ in $MgCl_2$ relative to that in NaCl correlates with the larger by ~18 kcal/mol overall enthalpy of its formation in this salt, $\Delta H_{obs} = 38.0\ (\pm 1.7)$ kcal/mol, as compared with that in NaCl, $\Delta H_{obs} = 20.4\ (\pm 2.1)$ kcal/mol. Similar difference between $\Delta H_{obs}$ in the two salt (~20 kcal/mol) was found in the case of RPo/Pa (cf. Table 1). Since both salts have common $Cl^-$ anion, $Mg^{2+}$ ions must thus play a major and specific role in the lowering of $|\Delta G_{298}|$ — most probably by enthalpy stabilization of the structure of one or both of the free components of RPo making thus the overall $\Delta H_{obs}$ more endothermic. Stabilization of RPo/$\lambda P_R$ in $MgCl_2$, without any significant change in $n_{obs}$, requires thus correspondingly higher entropy gain that can be achieved only in the lower range of [salt] than that observed in NaCl. On the other hand, the smaller $|\Delta G_{298}|$ value for RPo/$\lambda P_R$ in NaCl than in NaOAc at similar [salt] testifies that $OAc^-$ interacts weaker than $Cl^-$ with positively charged amino acid residues involved in electrostatic interactions with promoter phosphates at the DNA–RNAP interface, as it has been suggested earlier [6]. The overall enthalpy of RPo formation in NaOAc can be thus expected to be lower than that measured in NaCl. This remains to be tested experimentally.

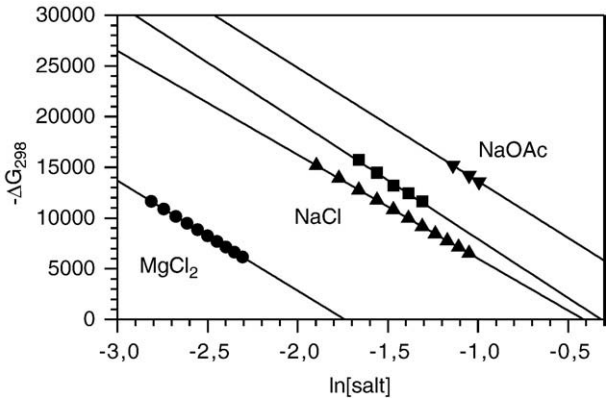


**Fig. 5.** Free energy, $\Delta G_{298}$, of RPo/$\lambda P_R$ formation at 298 K as a function of ln[salt]. In $MgCl_2$ (circles) and in NaCl (up triangles) calculated from corresponding $K_{obs}$ values (Table 1), and from the published data of Record laboratory [8,9]: in NaCl (rectangles) and NaOAc (down triangles). The small difference between $\Delta G_{298}$ values from the two laboratories can be due to somewhat different experimental conditions and methods of RPo quantification used in this work (MFDAI) and by the Record group (filter binding assay for $^3$H-labeled promoter DNA fragment).

What specific role can be played by $Mg^{2+}$ ions in the stabilization of the structure of one or both RPo components that makes the overall enthalpy of its formation more endothermic? It is well known that $Mg^{2+}$ ions, having by two-order of magnitude higher affinity to dsDNA as compared with that of monovalent $Na^+$ and $K^+$ [6,9,34,51], increase both dsDNA melting temperature and the corresponding [salt]-dependent free energy $|\Delta G_{T,salt}|$ [52–55]. Recent PAGE experiments of dsDNA molecules with solitary nicks and gaps [56] demonstrated that base-stacking is the main stabilizing factor in the dsDNA helix and that temperature- and [salt]-dependencies of this term determine the observed dependence of DNA stability on these variables. Nothing is known, however, about the effect of $Mg^{2+}$ on the enthalpy contribution to the free energy of DNA.

Information on how binding of $Mg^{2+}$ ions by free RNAP may affect its structure and thermodynamic stability is rather limited. It has been known since a long time that there is number of $Mg^{2+}$-binding sites on RNAP holoenzyme, among them one of a high affinity involved in the binding of NTP substrates [57,58], which may be identical with that of the RNAP catalytic center NADFDGD motif [42,59]. In the crystal structure of *T. thermophilus* RNAP multiple $Mg^{2+}$ ions were found to be located on the protein surface [59]. Since RNAP is an acidic protein these ions are presumably chelated to carboxylic groups located on the holoenzyme surface. We have found recently that RNAP in the presence of $Mg^{2+}$, both in the free and bound state in RPo, is strongly protected against $KMnO_4$ oxidation, probably owing to compaction and stabilization of its structure preventing thereby deeper penetration of $MnO_4^-$ anions to vulnerable amino acid residues [28]. Protection by $Mg^{2+}$ of *E. coli* RNAP holoenzyme from trypsin cleavage has been also earlier demonstrated [60].

### 4.3. Effect of promoter sequence on RPo stability

In both salts RPo/Pa is more stable than RPo/$\lambda P_R$ by a similar factor of $x_0(\mathrm{Pa})/x_0(\lambda P_R) = 1.2$ in spite of the fact that the overall unfavorable enthalpy of RPo formation at the Pa proved remarkably higher in either salt by as much as $\Delta\Delta H_{obs} \sim 30$ kcal/mol. The higher stability of RPo/Pa relative to that of RPo/$\lambda P_R$ in both salts is due to a large gain in entropy of $\Delta\Delta S_{obs,\ 1.0\ M} \sim 100$ e.u. For instance, at 0.1 M salt and 298 K the calculated difference in free energy between RPo/Pa and RPo/$\lambda P_R$ amounts to ca. −3.6 and −2 kcal/mol in NaCl and in $MgCl_2$, respectively. The higher values of thermodynamic functions: $\Delta H_{obs}$ and $\Delta S_{obs,\ 1.0\ M}$ and $|\Delta G_{obs,T}|$ correlate with $\Delta n_{obs} \approx +2$. (cf. Table 1). Since both promoters are located in the same region of the studied DNA fragment, the observed difference in thermodynamic stability of the respective complexes must be due to their different sequential structure (cf. Scheme 1).

The standard enthalpies of DNA melting, $\Delta H°$, calculated [61] for 14 bp (−11… +2) fragments of $\lambda P_R$ and Pa promoters: respectively as −113 and −105 kcal/mol, are much larger and in reverse order than the corresponding $\Delta H_{obs}$. For Pa, $\Delta H°$ is thus by 8 kcal/mol smaller than for $\lambda P_R$. Therefore, the $\Delta\Delta H_{obs} \sim 30$ kcal/mol difference between the two complexes cannot be related to the different stability of promoters' dsDNA in the transcription bubble region. For RPo/Pa, $\Delta\Delta H_{obs}$ correlates positively with $\Delta n_{obs} \approx +2$ both in NaCl and in $MgCl_2$. The latter difference is due primarily to the higher $n_a$ values (cf. Table 2). This may indicate formation of 2 additional ionic contacts and larger interface area between RNAP and Pa promoter in the $(I_1\text{–}I_2)^{\ddagger}$ state of the complex. Formation of additional contacts may contribute unfavorably to $\Delta H_{obs}$ owing to a higher refolding energy required for accommodation in RPo of the Pa promoter bearing canonical −10 and −35 hexamers and 17 bp AT-linker (cf. Scheme 1). Different overall vant'Hoff enthalpies found for RPo at other promoters: *lac*UV5 (70 ± 14 kcal, [25]) and *tetR* (40 kcal, [26]) can be attributed similarly to their particular sequential structure. Any reliable analysis of how the promoter sequence may affect mutually related folding processes of complex components on the path to RPo

and, consequently, also the overall enthalpy of the complex formation would require knowledge of its high resolution structure.

### 4.4. $Mg^{2+}$ effect on the rate of RPo dissociation in the presence of heparin

Heparin since a long time has been used as an effective polyanionic competitor of DNA for the discrimination between weak nonspecific and stronger specific DNA–RNAP complexes as well as in studies on kinetics of dissociation of the latter by rendering this process irreversible [6,8–10,16–19]. Weaker polymerase–promoter complexes are destroyed by bimolecular attack of heparin followed by DNA displacement. We have now shown that this is the case for RPo at the two studied promoters in $MgCl_2$ and that the bimolecular reaction is much less dependent on salt concentration than the true first-order rate of RPo dissociation. The large and apparently specific effect of heparin in the presence of $Mg^{2+}$ on the rate of RPo rises a question whether this effect is solely due to the lower stability of RPo in $MgCl_2$ or/and also to some specific effect of $Mg^{2+}$? As pointed out earlier in the Discussion, *E. coli* RNAP holoenzyme has a number of weak $Mg^{2+}$-binding sites in addition to that one of high affinity involved in catalysis and binding of NTP substrates [57,58]; also multiple $Mg^{2+}$ ions were found to be located on the surface of *T. thermophilus* RNAP in its crystal structure [59]. RNAP is an acidic protein so that it is highly likely that $Mg^{2+}$ binding sites are provided by carboxylic groups. One can thus envisage that $Mg^{2+}$ may facilitate direct attack of heparin on RPo by chelating $-COO^-$ groups on RNAP surface and thus lowering negative charge of the protein. Since effective charge of $Mg^{2+}$-chelated separated carboxylic groups is positive, heparin polyanions may accumulate around RNAP. Our observation that in the whole range of [$MgCl_2$] studied RPo did not form when RNAP was first incubated with heparin adds strength to this proposal. Heparin molecules bound dynamically to RNAP in RPo may migrate by fast surface diffusion to their ultimate targets *viz*. protein channels bearing template and nontemplate promoter strands causing displacement of one or both of them and thus destruction of the whole complex.

It should be recalled in this connection that enhanced binding of heparin to other proteins in the presence of $Mg^{2+}$ has been observed, for instance to endostatin [62] and to some membrane-bound heparin binding proteins [63].

## Acknowledgement

We thank Dr Jarosław Poznański for his help in visualization of and discussion on protein-DNA interactions.

## Appendix A. Interpretation of experimental binding isotherms for RPo

According to the theory of polyelectrolyte effect [5,7] at low to moderate salt concentrations the equilibrium constant of a protein–DNA complex is controlled primarily by ion-exchange processes with its components. In the case of RPo in a univalent salt solution, like NaCl, in principle both cations ($Me^+$) and anions ($A^-$) can be involved in salt-control of complex stability. Therefore, for RPo at equilibrium with its components:

$$\left(n_C Me^+\right)\mathrm{DNA} + (n_A A^-)\mathrm{RNAP} \Leftrightarrow \mathrm{RPo} + n_C Me^+ + n_A A^- \tag{A1}$$

the corresponding equilibrium constant can be written as:

$$K_{eq} = \frac{[\mathrm{RPo}] \times \left[Me^+\right]^{n_C} \times [A^-]^{n_A}}{[\mathrm{RNAP}] \times [\mathrm{DNA}]}. \tag{A2}$$

Under conditions of a large excess of RNAP over DNA concentration, [RNAP] ≫ [DNA], one can assume that [RNAP] does not change practically as the equilibrium of the reaction (A1) is shifted by variation in salt concentration, so that:

$$K_{eq} \times [RNAP] = \frac{[RPo] \times \left[Me^+\right]^{n_C} \times [A^-]^{n_A}}{[DNA]} = K. \tag{A3}$$

Measured by MFDAI fluorescence assay [RPo] is linearly proportional to the fluorescence intensity ($Y$) corrected for background emission ($Y2$):

$$[\mathrm{RPo}] \equiv Y - Y2 \tag{A4}$$

While [DNA] is proportional to the difference between a maximum value of the fluorescence signal ($Y1$) when all DNA is bound in RPo, and the measured one ($Y$):

$$[\mathrm{DNA}] \equiv Y1 - Y. \tag{A5}$$

Eq. (A3) can be thus rewritten as:

$$K = \frac{(Y - Y2) \times \left[\mathrm{Me}^+\right]^{n_C} \times [A^-]^{n_A}}{(Y1 - Y)} \tag{A6}$$

and transformed into the logarithmic form:

$$\ln K = \ln(Y - Y2) + n_C \times \ln\left[\mathrm{Me}^+\right] + n_A \times \ln[A^-] - \ln(Y1 - Y) \tag{A7}$$

and rewritten as:

$$\ln\frac{Y - Y2}{Y1 - Y} = \ln K - n_C \times \ln\left[\mathrm{Me}^+\right] - n_A \times \ln[A^-] \tag{A8a}$$

by setting $n_C + n_A = n_{obs}$, Eq. (A8a) can be simplified to read:

$$\ln\frac{Y - Y2}{Y1 - Y} = \ln K - n_{obs} \times \ln[\mathrm{Me}A]. \tag{A8b}$$

After antilogarithmic transformation and rearrangement one obtains:

$$Y = \frac{Y1 \times e^{(\ln K - n_{obs} \times \ln[\mathrm{Me}A])}}{1 + e^{(\ln k - n_{obs} \times \ln[\mathrm{Me}A])}} + Y2. \tag{A9}$$

After a number of algebraic rearrangements Eq. (A9) takes the following form:

$$Y = \frac{Y1 - Y2}{1 + e^{(n_{obs} \times \ln[\mathrm{Me}A] - \ln K)}} + Y2 \tag{A10}$$

Identical with the sigmoid Boltzman equation with ln[MeA] as an independent variable $x$ and parameters $\ln K / n_{obs}$ and $1 / n_{obs}$ set to $x_0$ and d$x$, respectively. Measured fluorescence intensity $Y$ (Eq. (A10)) corrected for background emission ($Y2$) and normalized relative to the maximal signal increment ($Y1 - Y2$), represents fractional occupancy of promoter DNA:

$$f_{\mathrm{RPo}} = \frac{Y - Y2}{Y1 - Y2} = \frac{1}{1 + e^{(n_{obs} \times \ln[\mathrm{Me}A] - \ln K)}}. \tag{A11}$$

Values of $Y1$ and $Y2$ can best be obtained by fitting the Boltzman function to the original fluorescence ($Y$,[salt]) data. Using fitted values of the ln$K$ and $n_{obs}$ parameters, and known concentration of active RNAP, the apparent equilibrium binding constant, $K_{obs,[\mathrm{Me}A],T} = \frac{[\mathrm{RPo}]}{[\mathrm{RNAP}] \times [\mathrm{DNA}]}$, at

any electrolyte concentration and temperature ($T$) can be estimated using the following expression:

$$\ln K_{\mathrm{obs},[\mathrm{Me}A],T} = \ln K_{\mathrm{eq},T} - n_{\mathrm{obs}} \times \ln[\mathrm{Me}A] = \ln K_T - \ln[\mathrm{RNAP}] - n_{\mathrm{obs}} \times \ln[\mathrm{Me}A]. \quad \text{(A12)}$$

Control calculations concerning the validity of the assumption underlying Eq. (A12), *viz.* that [RNAP] remains practically constant when used in a large excess over [DNA], have shown that at [RNAP]/[DNA] ≥ 10 is satisfactorily fulfilled since a ca. 10% change in [RNAP] would produce deviations in the values of fitted parameters within the limits of experimental error.

## References


[1] M.E. Maguire, J.A. Cowan, Magnesium chemistry and biochemistry, Biometals 15 (2002) 203–210.
[2] M.E. Maguire, Magnesium transporters: properties, regulation and structure, Front. Biosci. 11 (2006) 3149–3163.
[3] A. Sreedhara, J.A. Cowan, Structural and catalytic roles for divalent magnesium in nucleic acids biochemistry, Biometals 15 (2002) 211–223.
[4] V. Sosunov, E. Sosunova, A. Mustaev, I. Bass, V. Nikiforov, A. Goldfarb, Unified two-metal mechanism of RNA synthesis and degradation by RNA polymerase, EMBO J. 22 (2003) 2234–2244.
[5] M.T. Record Jr., J.-H. Ha, M.A. Fisher, Analysis of equilibrium and kinetic measurements to determine thermodynamic origins of stability and specificity and mechanism of formation of site-specific complexes between proteins and helical DNA, Methods Enzymol. 208 (1991) 291–343.
[6] S. Leirmo, M.T. Record Jr., Nucleic acids and molecular biology, in: F. Eckstein, D.M.J. Lilley (Eds.), Structural, thermodynamic and kinetic studies of the interaction of $E\sigma^{70}$ RNA polymerase with promoter DNA, vol. 4, Springer-Verlag, Berlin, Heidelberg, 1990, p. 123.
[7] M.T. Record Jr., W.S. Reznikoff, M.L. Craig, K.L. McQuade, P.J. Schlaz, *Escherichia coli* and *Salmonella*: cellular and molecular biology, in: F.C. Neidhardt (Ed.), *Escherichia coli* RNA Polymerase ($E\sigma^{70}$), Promoters, and the Kinetics of the Steps of Transcription Initiation, 2nd ed., ASM Press, Washington, D.C., 1996, pp. 792–820.
[8] J.-H. Roe, M.T. Record Jr., Regulation of the kinetics of the interaction of *Escherichia coli* RNA polymerase with the $\lambda P_R$ promoter by salt concentration, Biochemistry 24 (1985) 4721–4726.
[9] W.C. Suh, S. Leirmo, M.T. Record Jr., Roles of $Mg^{2+}$ in the mechanisms of formation and dissociation of open complex between *Escherichia coli* RNA polymerase and the $\lambda P_R$ promoter; kinetic evidence for a second open complex requiring $Mg^{2+}$, Biochemistry 31 (1992) 7815–7825.
[10] I.K. Kolasa, T. Łoziński, K.L. Wierzchowski, $Mg^{2+}$ does not induce isomerization of the open transcription complex of *Escherichia coli* RNA polymerase at the model Pa promoter bearing consensus −10 and −35 hexamers, Acta Biochim. Pol. 48 (2001) 985–994.
[11] R.R. Burgess, J.J. Jendrisek, A procedure for the rapid, large scale purification of *Escherichia coli* DNA-dependent RNA polymerase involving polyamine P precipitation and DNA-cellulose chromatography, Biochemistry 14 (1975) 4634–4638.
[12] T. Łoziński, K. Abdrch-Rożek, W.T. Markiewicz, K.L. Wierzchowski, Effect of DNA bending in various regions of a consensus-like *Escherichia coli* promoter on its strength in vivo and structure of the open complex in vitro, Nucleic Acids Res. 19 (1991) 2947–2953.
[13] T. Łoziński, K.L. Wierzchowski, $Mg^{2+}$ modulated $KMnO_4$ reactivity of thymines in the open transcription complex reflects variation in the negative electrostatic potential along the separated DNA strands. Footprinting of *Escherichia coli* RNA polymerase complex at the $\lambda P_R$ promoter revisited, FEBS J. 272 (2005) 2838–2853.
[14] M. Chamberlin, R. Kingstone, M. Gilman, J. Wiggs, A. DeVera, Isolation of bacterial and bacteriophage RNA polymerases and their use in synthesis of RNA in vitro, Methods Enzymol. 101 (1983) 540–568.
[15] L.R. Yarborough, J.G. Schlageck, M. Baughman, Synthesis and properties of fluorescent nucleotide substrates for DNA-dependent RNA polymerases, J. Biol. Chem. 254 (1979) 12069–12073.
[16] G. Walter, W. Zillig, P. Palm, E. Fuchs, Initiation of DNA-dependent RNA synthesis and the effect of heparin on RNA polymerase, Eur. J. Biochem. 3 (1967) 194–204.
[17] S.R. Pfeffer, S.J. Stahl, M.J. Chamberlin, Binding of *Escherichia coli* RNA polymerase to T7 DNA. Displacement of holoenzyme from promoter complexes by heparin, J. Biol. Chem. 252 (1977) 5403–5407.
[18] P.U. Giacomoni, E. Delain, J.B. Le Pecq, Electron microscopy analysis of the interaction between *Escherichia coli* DNA-dependent RNA polymerase and the replicative form of phage fd DNA. 2. Analysis of the dissociation kinetics, Eur. J. Biochem. 78 (1977) 215–220.
[19] C.L. Cech, W.R. McClure, Characterization of ribonucleic acid polymerase-T7 promoter binary complexes, Biochemistry 19 (1980) 2240–2247.
[20] SIGMA Product Information, Tris(hydroxymethyl)aminomethane, Tris. Sigma Technical Bulletin No. 106B, 1996.
[21] E. Stellwagen, O. Dong, N.C. Stellwagen, Quantitative analysis of monovalent counterion binding to random-sequence, double-stranded DNA using the replacement ion method, Biochemistry 46 (2007) 2050–2058.
[22] J.-H. Roe, R.R. Burgess, M.T. Record Jr., Temperature dependence of the rate constants of the *Escherichia coli* RNA polymerase–$\lambda P_R$ promoter interaction. Assignment of the kinetic steps corresponding to protein conformational change and DNA opening, J. Mol. Biol. 184 (1985) 441–453.
[23] O.V. Tsodikov, M.T. Record Jr., General method of analysis of kinetic equations for multistep reversible mechanisms in the single-exponential regime: application to kinetics of open complex formation between $E\sigma^{70}$ RNA polymerase and $\lambda P_R$ promoter DNA, Biophys. J. 76 (1999) 1320–1329.
[24] R.M. Saecker, L.M. McQuade, P.E. Schlax Jr., M.V. Capp, M.T. Record Jr., Kinetic studies and structural models of the association of *Escherichia coli* RNA polymerase with $\lambda P_R$ promoter: large scale conformational changes in forming the kinetically significant intermediate, J. Mol. Biol. 319 (2002) 649–671.
[25] H. Buc, W.R. McClure, Kinetics of open complex formation between *Escherichia coli* RNA polymerase and the lac UV5 promoter. Evidence for a sequential mechanism involving three steps, Biochemistry 24 (1985) 2712–2723.
[26] G. Duval-Valentin, R. Ehrlich, Dynamic and structural characterization of multiple steps during complex formation between *E. coli* RNA polymerase and tetR promoter from pSC101, Nucleic Acids Res. 15 (1987) 575–594.
[27] W.C. Suh, W. Ross, M.T. Record Jr., Two open complexes and a requirement for $Mg^{2+}$ to open the lambda PR transcription start site, Science 259 (1993) 358–361.
[28] T. Łoziński, K.L. Wierzchowski, Inactivation and destruction by $KMnO_4$ of *Escherichia coli* RNA polymerase open transcription complex; recommendations for footprinting experiments, Anal. Biochem. 320 (2003) 239–251.
[29] V. Tchernaenko, H.R. Halvorson, M. Kashlev, L.C. Lutter, DNA bubble formation in transcription initiation, Biochemistry 47 (2008) 1871–1884.
[30] S. Leirmo, C. Harrison, D.S. Cayley, R.R. Burgess, M.T. Record Jr., Replacement of potassium chloride by potassium glutamate dramatically enhances protein–DNA interactions in vitro, Biochemistry 26 (1987) 2095–2101.
[31] T.M. Lohman, P.L. deHaseth, M.T. Record Jr., Pentalysine–deoxyribonucleic acid interaction. A model for the general effects of ion concentrations on the interaction of proteins with nucleic acids, Biochemistry 19 (1980) 3522–3530.
[32] D.P. Mascotti, T.M. Lohman, Thermodynamics of single-stranded RNA and DNA interactions with oligolysines containing tryptophan. Effects of base composition, Biochemistry 32 (1993) 10568–10579.
[33] D.P. Mascotti, T.M. Lohman, Thermodynamics of oligoarginines binding to RNA and DNA, Biochemistry 36 (1997) 7272–7279.
[34] M.T. Record Jr., P.L. deHaseth, T.M. Lohman, Interpretation of monovalent and divalent cation effects on the lac repressor–operator interaction, Biochemistry 16 (1977) 4783–4791.
[35] M.W. Capp, D.S. Cayley, W. Zhang, H.J. Guttman, S.E. Melcher, R.M. Saecker, C.F. Anderson, M.T. Record Jr., Compensation effects of opposing changes in putrescine (2+) and $K^+$ concentrations on *lac* repressor–*lac* operator binding: *in vitro* thermodynamic analysis and *in vivo* relevance, J. Mol. Biol. 258 (1996) 25–36.
[36] V.K. Misra, K.A. Sharp, R.A. Friedman, B. Honig, Salt effects on ligand–DNA binding; Minor groove binding antibiotics, J. Mol. Biol. 238 (1994) 245–263.
[37] V. Misra, J. Hecht, K. Sharp, R. Friedman, B. Honig, Salt effects on protein–DNA interactions. The lambda cI repressor and EcoRI endonuclease, J. Mol. Biol. 238 (1994) 264–280.
[38] S.W. Chen, B. Honig, Monovalent and divalent salt effects on electrostatic free energies defined by the nonlinear Poisson–Boltzmann equation: application to DNA binding reactions, J. Phys. Chem. B 101 (1997) 9113–9118.
[39] G.-G. Cuauhtemoc, D.E. Draper, Electrostatic interactions in a peptide–RNA complex, J. Mol. Biol. 331 (2003) 75–88.
[40] P. Legault, J. Li, J. Mogridge, L.E. Kay, J. Greenblatt, NMR structure of the bacteriophage lambda N peptide/Box RNA comples: recognition of a GNRA fold by an arginine-rich motif, Cell 93 (1998) 289–299.
[41] K.S. Murakami, S. Masuda, E.A. Campbell, O. Muzzin, S.A. Darst, Structural basis of transcription initiation: an RNA polymerase holoenzyme–DNA complex, Science 296 (2002) 1285–1290.
[42] D.G. Vassylyev, M.N. Vassyleyeva, A. Perederina, T.H. Tahirov, I. Artsimovitch, Structural basis for transcription elongation by bacterial RNA polymerase, Nature 448 (2007) 157–162.
[43] S.P. Haugen, W. Ross, M. Manrique, R.L. Gourse, Fine structure of the promoter–σ region 1.2 interaction, Proc. Natl. Acad. Sci. U. S. A. 105 (2008) 3292–3297.
[44] T. Łoziński, K.L. Wierzchowski, $Mg^{2+}$ ions do not induce expansion of the melted DNA region of the open complex formed by *Escherichia coli* RNA polymerase at a cognate synthetic Pa promoter. A quantitative $KMnO_4$ footprinting study, Acta Biochim. Pol. 48 (2001) 495–510.
[45] V. Mekler, E. Kortkhonija, J. Mukhopadhyay, J. Knight, A. Rveyakin, A.N. Kapanidis, W. Niu, Y.W. Ebright, R. Levy, R.H. Ebright, Structural organization of bacterial RNA polymerase holoenzyme and the RNA polymerase–promoter open complex, Cell 108 (2002) 599–614.
[46] C. Wilson, A.J. Dombroski, Region 1 of $\sigma^{70}$ is required for efficient isomerization and initiation of transcription by *Escherichia coli* RNA polymerase, J. Mol. Biol. 267 (1997) 60–74.
[47] S. Vuthoori, C. Bowers, A. McCracken, A. Dombroski, D. Hinton, Domain 1.1 of the $\sigma^{70}$ subunit of *Escherichia coli* RNA polymerase modulates the formation of stable polymerase/promoter complexes, J. Mol. Biol. 309 (2001) 571–582.
[48] I. Rouzina, K. Pant, R.L. Karpel, M.C. Williams, Theory of electrostatically regulated binding of T4 gene 32 protein to single and double-stranded DNA, Biophys. J. 89 (2005) 1941–1956.
[49] L. Shokri, B. Marintcheva, C.C. Richardson, I. Rouzina, M.C. Williams, Single molecule force spectroscopy of salt dependent bacteriophage T7 gene 2.5 protein binding to single-stranded DNA, J. Biol. Chem. 281 (2006) 38689–38696.
[50] L. Shokri, B. Marintcheva, M. Elsib, A. Hanke, I. Rooouzina, M.C. Williams, Kinetics and thermodynamics of salt-dependent T7 gene 2.5 protein binding to single- and double-stranded DNA, Nucleic Acids Res. 36 (2008) 5668–5677.

[51] H.S. Strauss, R.R. Burgess, M.T. Record Jr., Binding of *Escherichia coli* ribonucleic acid polymerase holoenzyme to a bacteriophage T7 promoter-containing fragment: evaluation of promoter binding constants as a function of solution conditions, Biochemistry 19 (1980) 3504–3515.
[52] S. Nakano, M. Fujimoto, H. Hara, N. Sugimoto, Nucleic acid duplex stability: influence of base composition on cation effects, Nucleic Acids Res. 27 (1999) 2957–2965.
[53] J. SantaLucia Jr., D. Hicks, The thermodynamics of DNA structural motifs, Ann. Rev. Biophys. Biomol. Struct. 33 (2004) 415–440.
[54] N. Korolev, A.P. Lyubratsev, L. Nordenskiöld, Application of polyelectrolyte theories for analysis of DNA melting in the presence of $Na^{+}$ and $Mg^{2+}$ ions, Biophys. J. 75 (1998) 3041–3306.
[55] Z.-J. Tan, S.-J. Chen, Nucleic acid helix stability: effects of salt concentration, cation valence and size, and chain length, Biophys. J. 90 (2006) 1175–1190.
[56] P. Yakovchuk, E. Protozanova, M.D. Frank-Kamenetskii, Base-stacking and base-pairing contributions into thermal stability of the DNA double helix, Nucleic Acids Res. 34 (2006) 564–574.
[57] R. Koren, A.S. Mildwan, Magnetic resonance and kinetic studies of the role of divalent cation activator of RNA polymerase from *Escherichia coli*, Biochemistry 16 (1977) 241–249.
[58] P. Szafrański, J.W. Smagowicz, K.L. Wierzchowski, Substrate selection by RNA polymerase from *E. coli*. The role of ribose and 5'-triphosphate fragments, and nucleotide interaction, Acta Biochim. Pol. 32 (1985) 329–349.
[59] D.G. Vassylyev, S.-I. Sekine, O. Laptenko, J. Lee, M.N. Vassyleyeva, S. Burukhov, S. Yokoyama, Crystal structure of bacterial polymerase holoenzyme at 2.5 A resolution, Nature 417 (2002) 712–719.
[60] R. Fisher, T. Blumenthal, Analysis of RNA polymerase by trypsin cleavage, J. Biol. Chem. 255 (1980) 11056–11062.
[61] J. SantaLucia, H.T. Allawi, P.A. Seneviratne, Improved nearest-neighbor parameters for predicting DNA duplex stability, Biochemistry 35 (1996) 3555–3562.
[62] S. Ricard-Blum, O. Féraud, H. Lortat-Jacob, A. Rencurosi, N. Fukai, F. Dkhissi, D. Vittet, A. Imberty, B.R. Olsen, M. van der Rest, Characterization of endostatin binding to heparin and heparin sulfate by surface plasmon resonance and molecular modeling. Role of divalent cations, J. Biol. Chem. 279 (2004) 2927–2936.
[63] K. Imai, T. Iida, Y. Takano, N. Uozumi, Membrane-bound heparin binding proteins from HL-60 cells purified in a two-step affinity chromatography differentially with divalent cations, J. Chromatogr., B, Biomed. Sci. Appl. 780 (2002) 1–12.